

The Design of a Droop-based Grid Forming Inverter Controller for Different Operation Modes and Conditions

Dalia Salem*, Detlef Schulz

Department of Electrical Power Systems

Helmut-Schmidt-University / University of the Federal Armed Forces Hamburg

Hamburg, Germany

* dalia.salem@hsu-hh.de

Abstract – Many countries are adopting strategies to base their electricity supply on 100 % renewable energy sources before the year 2050. To reach this goal, conventional power systems will be phased out and replaced by all types of renewable energy sources such as photovoltaics, wind turbines, hydroelectric power, geothermal energy accompanied by supportive systems for energy storage. The increasing share of renewable energy sources requires an accurate analysis of the behavior of each component in these systems in different system topologies and conditions. The main component that represents the interface connecting these sources to the grid or to different loads is the controllable inverter. This paper discusses a control technique for the inverter controller and analyses its behavior in the two operating modes grid-connected and island mode and also during transitions between these modes. In the process the system will follow not only steady state operation but also experience fault events. In this article, various models are built and discussed to investigate their transient behavior and dynamics.

Keywords— *Island mode, grid-connected operation mode, grid-forming inverters, cascaded control loops, decoupled frequency and voltage control.*

NOMENCLATURE

| | |
|------------|--|
| CoupleIT! | IT-gestützte Sektorenkopplung: Digital gesteuerte Brennstoffzellen- und Elektrolysetechnologie für stationäre und mobile Anwendungen |
| EES | Electrical energy storage |
| EMC | Electromagnetic compatibility |
| GFM | Grid-Forming Inverter |
| IGBT | Insulated-gate bipolar transistor |
| PID | Proportional–Integral–Derivative Controller |
| PQ | Active power–Reactive power |
| PV | Photovoltaic |
| PWM | Pulse width modulation |
| SiC-MOSFET | Silicon Carbide metal–oxide–semiconductor field-effect transistor |
| SVPWM | Space Vector Pulse Width Modulation |

| | |
|-----|--------------------------|
| VF | Voltage-Frequency |
| VSC | Voltage source converter |

I. INTRODUCTION

Due to the increasing interest in converter-based technologies, many projects are released to study the combination of this new technology with the old ones and also to build up a pure 100 % converter-based grids. In these power systems, the interconnected inverters have to show a certain behavior to achieve the required stability in a short timescale. For these systems, new operating conditions are defined based on the used type of the inverter. These inverters, which are known as Grid-Forming Inverters (GFM), are considered the dynamics leaders in a microgrid and they are forming the microgrid robustness against stability issues. They deal with short term dynamics, which are happening periodically and they have to keep tracking the new requirements in a very short time bandwidth. In conventional power systems, the synchronous generator dominates the short-term stability behavior with their electromechanical characteristics. In inverter-based power systems, the inverter emulates the response, dynamics and role of the synchronous generator [1], therefore the need for examining the system stability for a very short-term period increase. Then, the characteristics of such converters and their classifications and also their function in the microgrid have to be investigated to reach for the proper control technique for the proposed controllers. The type of the converter used to fulfill the grid forming function in a microgrid is a voltage source converter (VSC). GFMs are needed to be able to access a dispatchable power source, then they are able to provide a reliable operation. A GFM inverter is required to form and set the grid voltage magnitude and frequency and keeps it almost constant against harmful unexpected transient, keeps the system connected to avoid any shedding or trips. The main contribution of this manuscript is about a proposed control technique for a GFM inverter and can be summarized as follows: a short description for the IT-gestützte Sektorenkopplung: Digital gesteuerte Brennstoffzellen- und Elektrolysetechnologie für stationäre und mobile Anwendungen (CoupleIT!) project inverter, then an analytic section of the proposed controller loops, it is followed by some case studies to check this controller behavior in many operational situations and finally a short mention of the next step for this work and a summarized conclusion.

II. COUPLE-IT! DC/AC CONVERTER TOPOLOGY

Many projects nowadays based on converters, especially GFM are taking place in Australia, Scotland [1], USA and Germany. This trend is getting wider because of the recent environment acceleratory critical situation and a certain need to exclude the old power systems, which are one of the harmful main factors that affect our climate. In the Couple-IT! project, the main plan is to form a microgrid to be able to operate when grid-connected and also when stand alone. The selected inverter in the project is a three-phase, three-leg module DC/AC converter connected with a three-phase set of a passive LC filter at its output terminals. The proper selection of the inverter configuration is considered a challenge itself at the design phase. There are many offered inverter topologies and the differences between these topologies can be summed up in: the implemented pulse width modulation (PWM) level, the number of the inverter legs and the type of the series-connected filter at its output [1]. The common switching semiconductor used in these inverters are the Insulated-gate bipolar transistors (IGBT) [1]. In Couple-IT project the required inverter specifications are fulfilled by a two-level, three-legs, three-phase inverter with Silicon Carbide metal-oxide-semiconductor field-effect transistors (SiC-MOSFET), which provides high switching frequency, minimize the sizing issues and reduces the conducting losses, which is been manufactured by Imperix and shown in FIGURE 1 [2]:

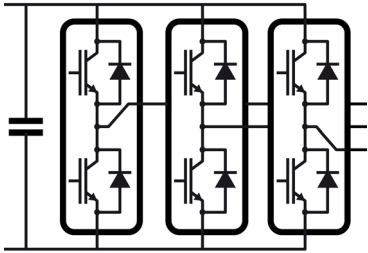


FIGURE 1: THREE-PHASE, TWO LEVEL IMPERIX INVERTER “ADAPTED FROM IMPERIX DATA SHEET”.

This inverter is connected via a DC/DC converter to a battery source; hence it operates as a VSC. Depending on the required application, the number of the inverter legs is selected.

As for the inverter levels, the implemented inverter in the project Couple-IT is a two-levels inverter, which is the most common type [1]. A multi-level inverter introduces a smoother waveform, and the more level numbers are included, the smoother the output waves are going to be. In this type, the two switching elements in any leg switch consecutively, not simultaneously to avoid the short circuit fault at the DC source terminals. Each leg of the inverter has a two-level state [1]. The three-level inverter achieves a better-quality performance and in higher power applications, which is classified to be more than 30 kW, it reduces also the filter size compared to the two-level inverter [1]. According to the IEEE-519 standard [1], there are certain constraints for the allowed harmonics in the output waves. The used pulse width modulation technique is the Space Vector Pulse Modulation (SVPWM) to determine the generated modulated signals for the inverter switches. One of the great benefits of this scheme is its low harmonic content in the generated sine waves. The implanting of a filter at the inverter output terminals become a fixed requirement to avoid high harmonic distortion effect. The selected filter topology has to fulfill the optimum elimination of different harmonics orders with considering the

bulky filter size to be avoided. The selected filter is an electromagnetic compatibility (EMC) Filter for both Photovoltaic (PV) and battery inverters.

III. CONTROL STRATEGY OF GFM INVERTER

First, the main functions of the GFM have to be well defined. GFM are responsible for [1] [3]:

- Set the voltage magnitude and the frequency of the microgrid, while operating in the islanding mode.
- Achieve a successful synchronization with the main grid, while grid-connected.
- Grid-connected or island detection and stable operation and transition.
- Keep the system intact while disturbances and not to loss stability.

The designed controller has to fulfill all these demands, while single-unit operated and also when parallel-operated. And since the control topology is planned to control a voltage source converter, which means it has to provide a fast time response to any disturbance. All of these demands have to be considered.

The control topology in a microgrid control hierarchy is based on three levels [3], as shown in FIGURE 2, the primary level which involves the data acquisition phase by measuring and voltage/frequency control and setting the reference bases as well. In the secondary level, the required measures are taken to restore the frequency and voltage at the standardized values and also the real time compensations are taken place in this control level. At the tertiary control level, the optimal system energy is managed and the power flow is controlled as well. The proposed controller is designed based on guarantee the first two levels to be achieved and fulfilled. In other words, both the primary and secondary control are examined during the controller operation.

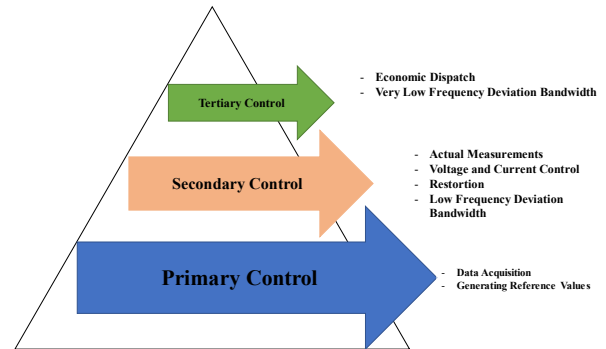


FIGURE 2: MICROGRID CONTROL HIERARCHY.

In this section, the proposed cascaded-loops controller shown in FIGURE 3 is explained in detail and the illustrated results are obtained from examining it with MATLAB-Simulation tool. The first input stage at the proposed controller is the “Data Acquisition” phase, where the voltage V_{pcc} (three-phase voltage signal at the common coupling point) is measured online and the reference active power, reference reactive power and reference frequency signals are generated. The reference voltage signal is also generated by comparing V_{pcc} to the nominal voltage and the error signal feeds a PI controller with the mentioned coefficients as in TABLE I.

TABLE I.: THE PROPOSED CONTROLLER LOOPS PARAMETERS.

| Controller Parameters | | | |
|-------------------------|-------|------------------------|------|
| Parameter | Value | 2)Voltage Control Loop | |
| f_{nom} | 50 Hz | K_p | 0.1 |
| V_{nom} | 400 V | K_i | 7 |
| V_{dc} | 800 V | 3)Active power PID | |
| Data Acquisition | | K_p | 0.03 |
| 1)Frequency regulator | | K_i | 2 |
| K_p | 0.03 | K_d | 13 |
| K_i | 2 | 4)Reactive power PID | |
| 2)Voltage regulator | | K_q | 3 |
| K_{qd} | 8 | K_{pv} | 0.52 |
| K_{qi} | 10 | K_{iv} | 1.16 |
| Cascaded Control Loops | | 3)Current Control Loop | |
| 1)Damping Resistor Loop | | K_{pc} | 0.73 |
| R_v | 0.09 | K_{ic} | 1.19 |

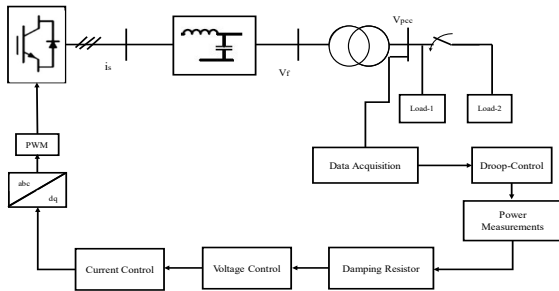


FIGURE 3: GRID-FORMING PROPOSED CONTROLLER CASCADED LOOPS.

As for generating the reference active power [4] and reactive power, two loops of PID controllers connected to the output error of nominal frequency and measured frequency and the error of the nominal voltage and measured voltage, as shown in FIGURE 4, 5.

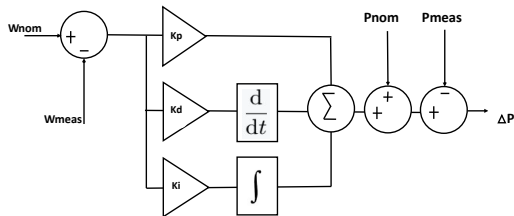


FIGURE 4: PID FOR ACTIVE POWER REFERENCE GENERATION.

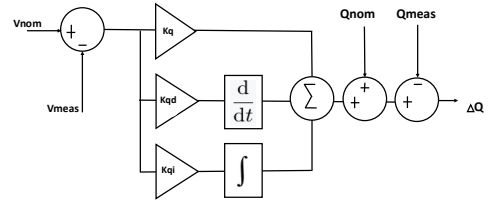


FIGURE 5: PID FOR REACTIVE POWER REFERENCE GENERATION.

The second phase is the measurements. The active and reactive power signals are calculated from the three phase measured voltages and currents. The third stage is the initialization phase, where the dq0 values from “ i_s , V_f ” and both the i_{d_ref} , i_{q_ref} signals are generated to feed the cascaded structure of the controller [4] [8], which is consisting of three main control loops. The first loop is called “Damping Resistor”, as shown in FIGURE 6.

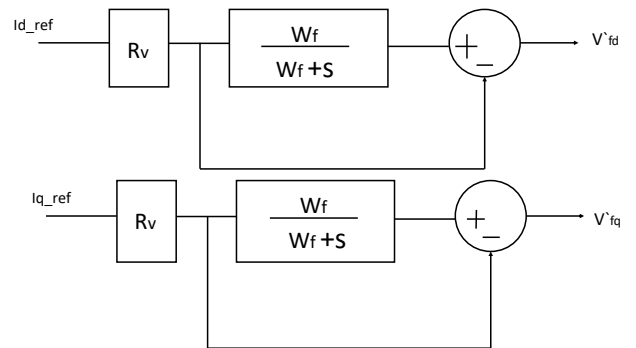


FIGURE 6: DAMPING RESISTOR CONTROL LOOP.

The output signals of this loop are going to feed the voltage control loop, which is shown in FIGURE 7.

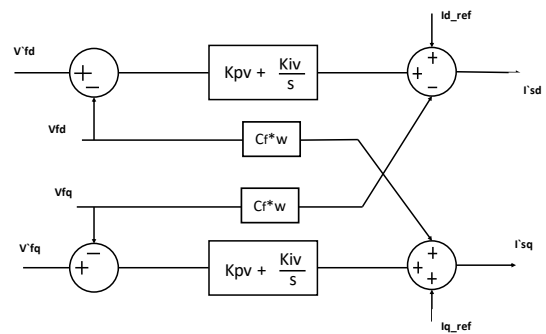


FIGURE 7: VOLTAGE CONTROL LOOP.

The output signals from this loop feed the current control loop as shown in FIGURE 8.

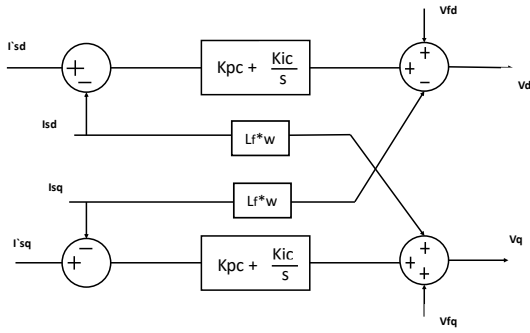


FIGURE 8: CURRENT CONTROL LOOP.

The final stage is to generate the pulses which trigger the inverter switches.

The robustness of this controller is tested to check its performance against load variations, severe condition and smooth transition between operating modes and if it can fulfill the control requirements, which are mentioned previously.

It has to be mentioned that, this controller is tested with MATLAB/Simulink tool and is going to be tested later in the Imperix inverter itself.

IV. CASE STUDY(1): SINGLE DROOP-BASED GRID FORMING CASE STUDY:

The purpose of this analysis is to examine if the inverter is able to create the microgrid, feed the load and cope with different changes, the small changes and the sever ones without losing its stability and keeping the system connected. The shown system in FIGURE 9 is used to test the designed controller during starting up the operation and during load variation.

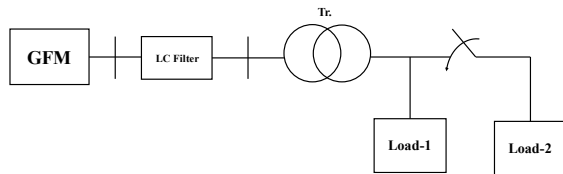


FIGURE 9: SINGLE-LINE DIAGRAM OF A STANDALONE GRID-FORMING INVERTER.

The two base lines to describe the droop control are: when the drawn active power increases, the frequency drops instantly and vice versa and the drawn power increases with a step response [6]. In this operation case, the inverter is operated in a Voltage-Frequency (VF) mode [7], which is another way to name its function as a responsible for setting the microgrid voltage and frequency. At $T=0$ sec., the system starts and it is observed how the controller set the nominal frequency and voltage of the grid and how it responds once the fluctuations start and acts on suppressing them, as shown in FIGURE 10.

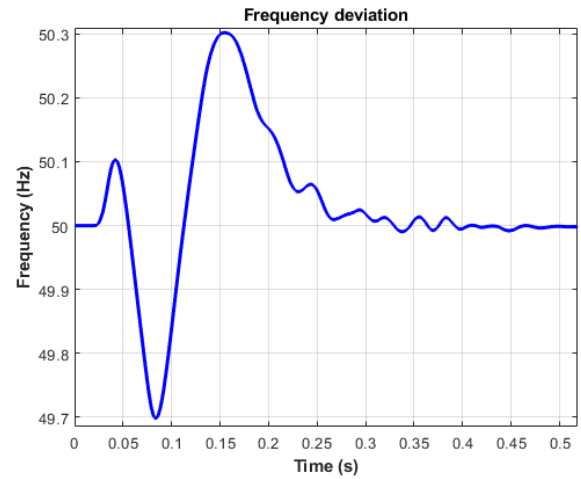


FIGURE 10: GFM INVERTER FREQUENCY RESPONSE AT START-UP.

After about 0.25 sec., the system can settle down at 50 Hz and the controller can damp the resulted oscillations. It is also noticeable the similar behavior above and below the setting 50 Hz value, which is like the synchronous generator response when starting to operate. At $T=1$ sec., load 2 is applied and removed again at $T=5$ sec. and the controller respond at once with the shown step increase and decrease in the active and reactive powers responses in FIGURE 11, 12:

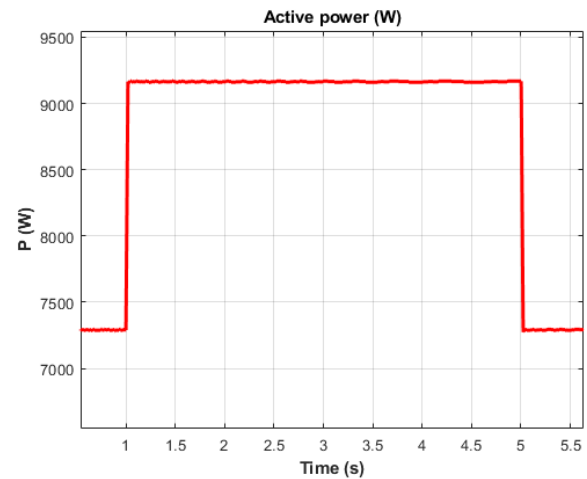


FIGURE 11: ACTIVE POWER STEP RESPONSE TO A LOAD-JUMP AND REMOVE.

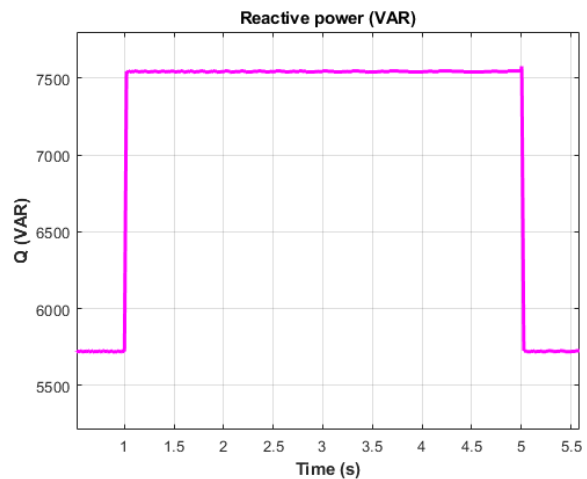


FIGURE 12: REACTIVE POWER STEP RESPONSE TO A LOAD-JUMP AND REMOVE.

The system frequency copes up with these variations with a decrease below 50 Hz when the powers increase and a rise up when the power decreases, as shown in FIGURE 13,14:

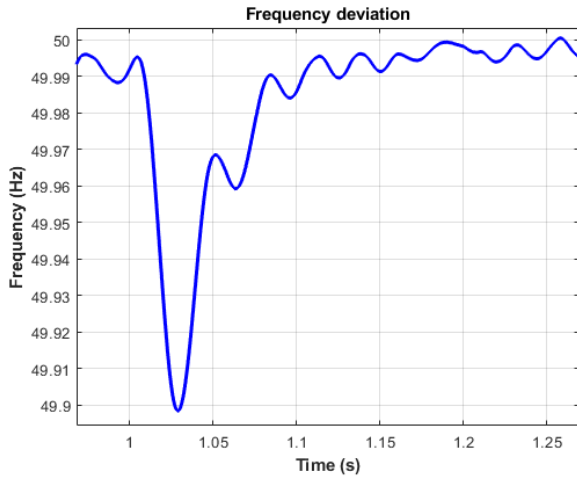


FIGURE 13: FREQUENCY DECREASE IN RESPONSE TO A LOAD JUMP.

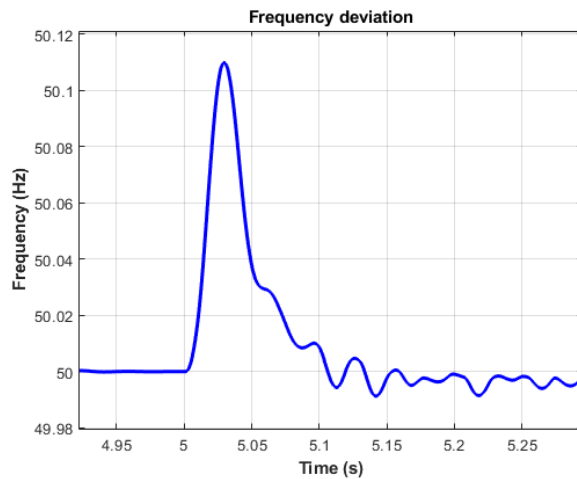


FIGURE 14: FREQUENCY INCREASE IN RESPONSE TO A LOAD DECREASE.

As shown in this model, the controller can compensate quickly for the sudden needed raise of powers and also restore the system steady state point.

The same system is going through two more expected operation conditions, the first one when it is hit by a severe fault and the second one the transition between modes of operations.

The controller is tested against a sudden 3-phase short circuit, which is the most severe fault can hit a power system. At $T=1$ sec., a 3-phase short circuit hits the stand-alone microgrid and it lasted for 0.01 sec. before it is completely isolated, the controller responds in the shown way in FIGURE 15.

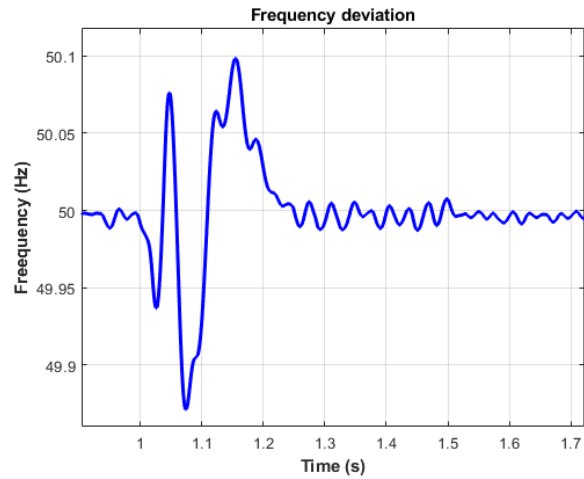


FIGURE 15: FREQUENCY OSCILLATORY RESPONSE TO A 3PHASE FAULT.

The controller survives the fault and can damp the frequency oscillations in a perfect timing and the system does not lose its stability.

Then the controller is tested through switching between islanded-mode to grid-connected load to examine its ability to achieve smooth transition and be synchronized successfully with the main power grid.

Smooth transition means that the voltage magnitude and phase and the frequency are not changing rapidly or beyond the setting limits at the instant of transition [7]. Consequently, the load receives a continuously uninterrupted power and the transient current is limited [7].

At $T=2$ sec., the system shown in FIGURE 16, changes its status from islanded mode to grid-connected.

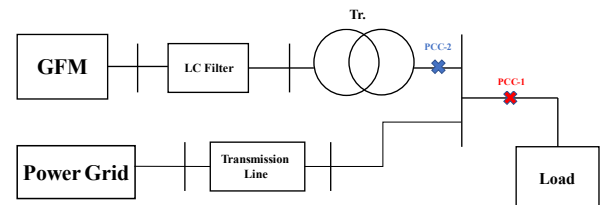


FIGURE 16: SINGLE-LINE DIAGRAM OF A STANDALONE GRID-FORMING INVERTER.

Now, the main grid is responsible for setting the system nominal frequency and voltage. The frequency variation is shown in FIGURE 17.

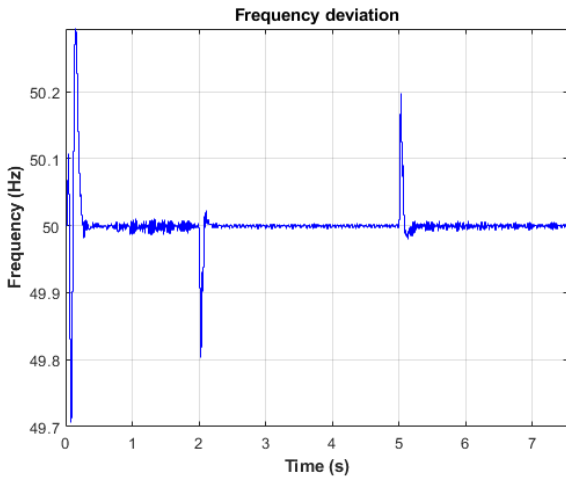


FIGURE 17: FREQUENCY RESPONSE AT GRID-CONNECTED INSTANT AND 2ND ISLAND.

And the input voltage at the load terminals at the measuring point PCC-1 will be as in FIGURE 18, which shows the slight change in the applied voltage while transferring from island mode to grid-connected and to island mode once more:

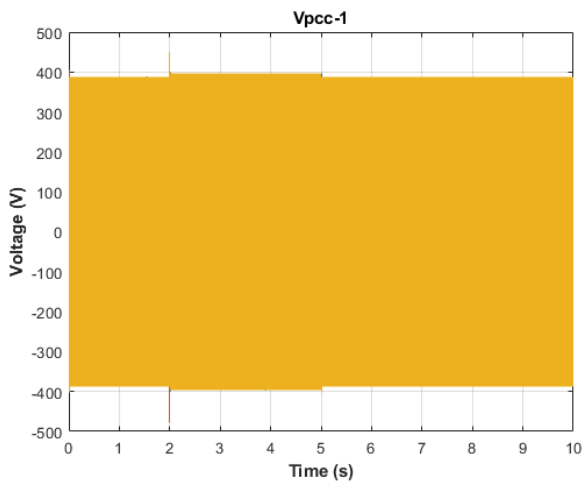


FIGURE 18: OUTPUT VOLTAGE WHEN CHANGING MODES AT PCC-1.

The supplied current to the load injected at PCC-1 is kept almost the same without suffering from high inrush currents at the instant of mode changing, as seen in FIGURE 19:

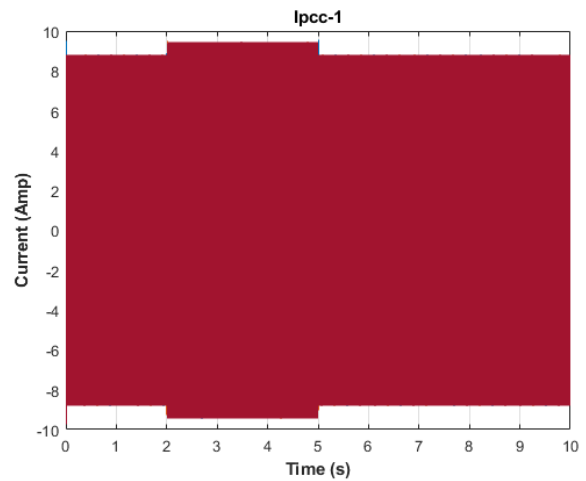


FIGURE 19: OUTPUT CURRENT WHEN CHANGING MODES AT PCC-1.

The inverter, while standing alone, is responsible for setting the system voltage. Once the main grid is connected, it rules the voltage magnitude. The controller can achieve successful synchronization with the main grid. GFM inverter should have the ability to inject or absorb a scheduled amount of active and reactive powers when they are grid connected. At $T=5$ sec., the controller is able to detect the absence of the main grid and can establish the island operational conditions, the voltage and frequency, at once and re-injecting the required active and reactive powers. In FIGURES 20 and 21, and at the measuring point PCC-2 at the GFM terminals, the GFM active and reactive power share, when grid-connected and when it is operated as a stand-alone unit again, are shown. As in FIGURE 20, once the main grid dominates the operation, it feeds the load and supplies the microgrid itself besides the losses.

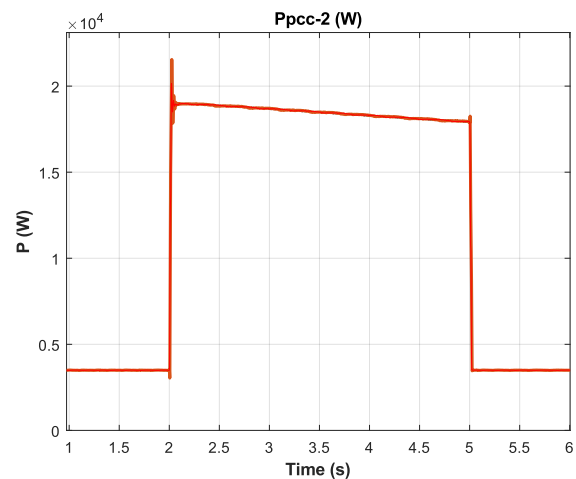


FIGURE 20: OUTPUT ACTIVE POWER WHEN CHANGING MODES AT PCC-2.

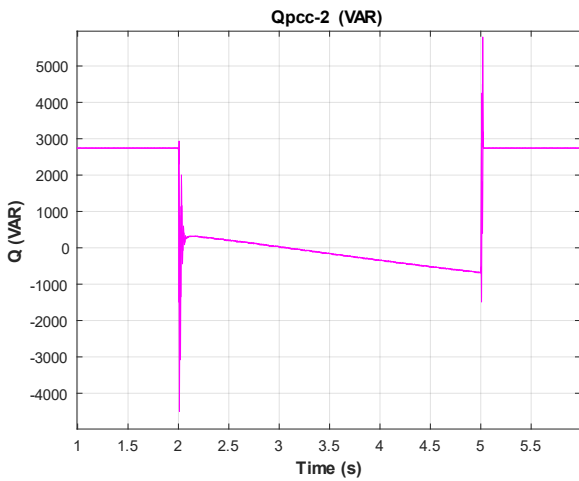


FIGURE 21: OUTPUT REACTIVE POWER WHEN CHANGING MODES AT PCC-2.

The controller can achieve the required power tracking in both operation modes. In this mode, the inverter is operated in the Active power-Reactive power (PQ)-Mode [8]. The controller has the flexibility and reliability to change between VF-Mode and PQ-Mode.

As it shown in the results, the microgrid goes through a smooth transition between modes.

The following case study is to examine the controller behavior during the parallel operation with another droop-based unit in island-mode.

V. CASE STUDY (2): PARALLEL OPERATION OF TWO DROOP-BASED GRID-FORMING CONVERTERS:

This case study is carried out to test some operational concepts between the two parallel units, such as the load sharing and how the dominance of the voltage source nature of the grid-forming inverter has a remarkable effect on the microgrid while standing-alone stability. The voltage source nature of the GFM inverters makes it able to generate a stable microgrid and achieve almost fixed voltage and frequency to build it up. The power system, shown in FIGURE 22, is simulated in many conditions to test the controller functionality in parallel-operation.

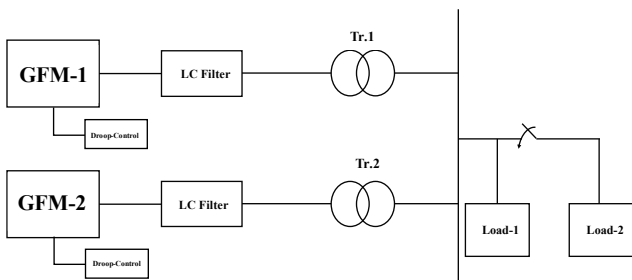


FIGURE 22: PARALLEL OPERATION OF 2 GRID-FORMING UNITS.

As for the first grid-forming unit, its rated power is 10 kW and its frequency-droop coefficient is 1 % and voltage-droop coefficient is 4 %. While the other unit is a droop-based grid-forming controlled inverter with a 10 kW as its rated power and the same droop coefficients. The system is hit with a sudden load increase lasts for six seconds before it is removed

again. The total load is shared between the two units as shown in FIGURE 23, 24:

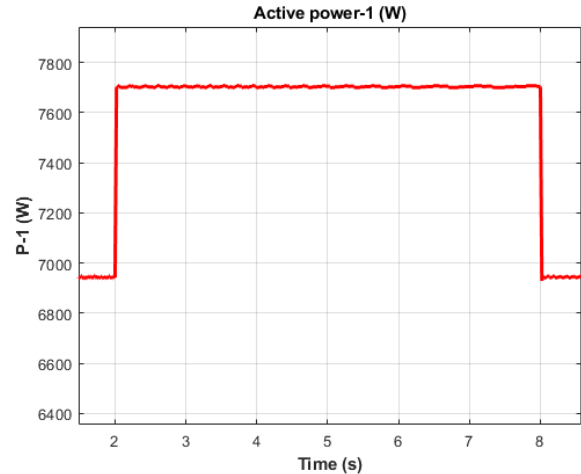


FIGURE 23: FIRST UNIT POWER INSTANTANEOUS COPING WITH A LOAD-JUMP AND REMOVE.

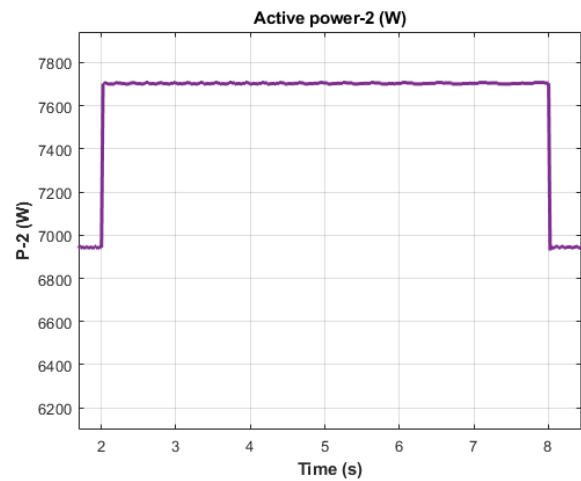


FIGURE 24: FIRST UNIT POWER INSTANTANEOUS COPING WITH A LOAD-JUMP AND REMOVE.

In FIGURE 25, the system as an integrated one-unit frequency response is shown.

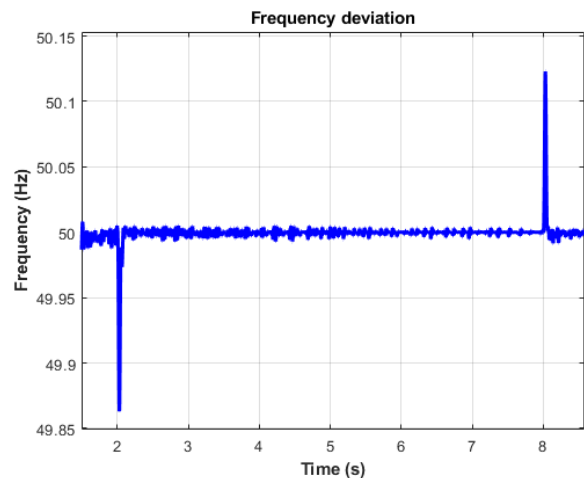


FIGURE 25: SYSTEM FREQUENCY IN RESPONSE TO LOAD VARIATIONS.

The same model is re-simulated this time to test it when black starting and when Load-1 is applied to its terminals, when the droop coefficient of the second unit changes to be 2 %, while the first still is 1 %. The first unit rated power is now 15 kW, but the second one is 10 kW and 4 % voltage droop. The main purpose of doing such analysis, is to test the rated limits of each unit when they start as a black started grid and how the droop coefficient and its rated power can affect its power share when starting-up and examine the maximum limit of each unit at the starting instant. The simulated system is shown in FIGURE 26.

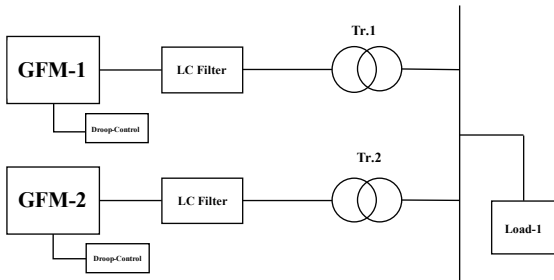


FIGURE 26: 2-PARALLEL CONNECTED GFMS WHEN BLACK-STARTING.

At one hand, at the startup instant, the first unit takes the larger share of the system loading as shown in FIGURE 27:

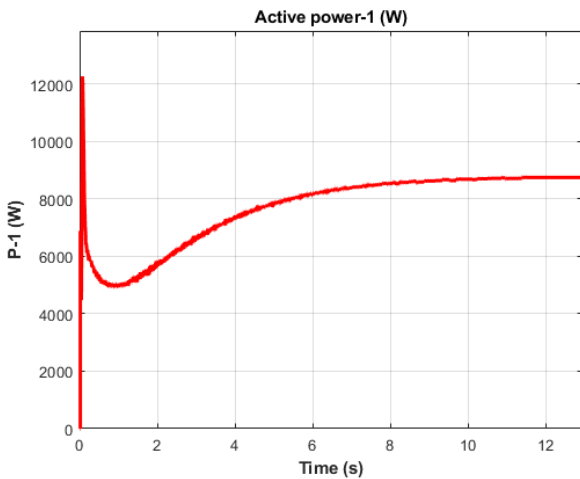


FIGURE 27: FIRST UNIT POWER SHARE.

On the other hand, at the same instant, the second unit is loaded with the smaller amount of the system loading as shown in FIGURE 28:

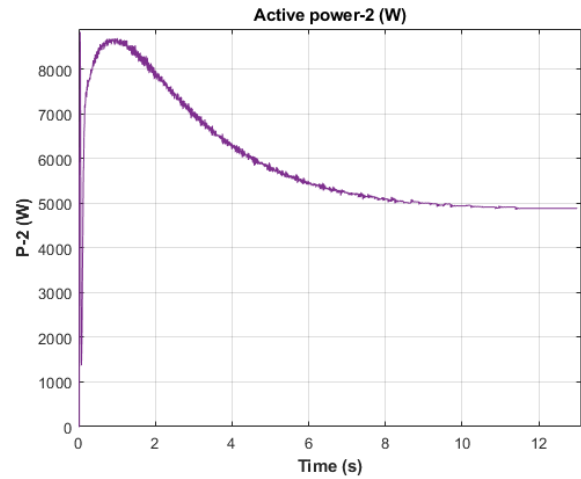


FIGURE 28: SECOND UNIT POWER SHARE.

This model shows a very interesting behavior of this parallel system, which is quite similar to the synchronous generators-based systems behavior. In conventional power systems, the initial load sharing and re-sharing depends on the inertia of each machine and the synchronizing power for soft and rigid machines [9][10]. Here in this system, which 100 % converter-based, the initial share is not the final load distribution among the parallel units. As shown in FIGURES 27 and 28, the first unit at the startup instant, the one with higher rated nominal power and smaller frequency droop coefficient, takes the larger share of loading. Simultaneously, the second unit takes the less portion of the initial loading. In this millisecond period, the load sharing depends on the rated power of each unit. Then a re-distributing for the load takes place between the two parallel units and the first unit drops some of the loading to be fed by the second unit until both units settle down to a steady power share. The final larger load portion is taken by the first unit.

VI. FUTURE WORK

Future work will deal with the combination of this droop-based converter with a DC/DC bidirectional converter that itself is connected to the battery source (EES) and the development of a proper control technique for this DC/DC converter as a step towards a comprehensive energy management system. Furthermore, the simulation results for the controller proposed will be validated in the laboratory by implementing the control scheme in our Imperix inverter. Another area of interest is the operation of this proposed controller in parallel with a grid-following inverter while operating in island mode.

VII. CONCLUSION

A valid controller has to i) fulfil the required standardized control functions, ii) be reliable under varying operating conditions, and iii) survive any power system incident in order to achieve the desired goal of maintaining a system's stability. The results show that the proposed controller is capable of fulfilling those tasks. In island-mode it is able to generate and keep the system voltage and frequency. It also achieves power tracking in both modes of operation: island mode and grid-connected mode. Moreover, the controller facilitates a smooth and reliable transition between those modes. As a result, the chosen control strategy guarantees stable operation in all of the tested operating modes and conditions.

VIII. ACKNOWLEDGEMENT

This research is part of the project ‘IT-gestützte Sektorenkopplung: Digital gesteuerte Brennstoffzellen- und Elektrolysetechnologie für stationäre und mobile Anwendungen – CoupleIT!’ that is funded by dtec.bw — Digitalization and Technology Research Center of the Federal Armed Forces of Germany, which we gratefully acknowledge.

REFERENCES

- [1] S. Anttila, J. Döhler, J. Oliveira and C. Boström, “Grid Forming Inverters: A Review of the State of the Art of Key Elements for Microgrid Operation”, *Energies* 15, 5517, 2022.
- [2] N. Cherix, “Power Electronic Building Blocks”, Imperix, Switzerland, 2020.
- [3] X. Zhang, A. Ukil, “Enhanced Hierarchical Control of Hybrid EnergyStorage System in Microgrids”, *IECON 2018 - 44th Annual Conference of the IEEE Industrial Electronics Society*, Washington, DC, USA, 30. Dec. 2018, 18382337.
- [4] D. S. Junior, J. Dohler, P. Almeida, J. de Oliveira, “Droop Control for Power Sharing and Voltage and Frequency Regulation in Parallel Distributed Generations on AC Microgrid”, *INDUSCON 13th IEEE International Conference on Industry Applications*, Sao Paulo, Brazil, 2018, 18438141.
- [5] K. Joung, T. Kim and J. Park, “Decoupled Frequency and Voltage Control for Stand-Alone Microgrid with High Renewable Penetration”, *54th IEEE/IAS Industrial and Commercial Power Systems Technical Conference (I&CPS)*, Niagara Falls, ON, Canada, 31 May 2018, 17805704.
- [6] J. Wang, “Design Power Control Strategies of Grid-Forming Inverters for Microgrid Application”, *2021 IEEE Energy Conversion Congress and Exposition (ECCE)*, Vancouver, BC, Canada, 16. Nov. 2021, 21299291.
- [7] S. Mansour, M. Marei and A. A. Sattar, “Droop based Control Strategy for a Microgrid”, *Global Journal of Researches in Engineering: F, Electrical and Electronics Engineering*, Global Journals Inc. USA, 2018, 2249-4596 .
- [8] E. Rokrok, T. Qoria, A. Bruyere, B. Francois, X. Guillaud, “Classification and Dynamic Assessment of Droop-Based Grid-Forming Control Schemes: Application in HVDC Systems”, *21st Power Systems Computation Conference, PSCC 2020*, Porto, Portugal, July 2020.
- [9] R. Rudeubenburg, "Transient performance of electrical power system", *The M.I.T. Press*, Cambridge, Mass, 1969.
- [10] M. Eremia, M. Shahidehpour, "Handbook of ElectricalPower System Dynamics", *IEEE Press Editorial Board*, Wiley & Sons, Incorporated, John, 2013.